AUTOMATIC RETRIEVAL OF CROP CHARACTERISTICS: AN EXAMPLE FOR HYPERSPECTRAL AHS DATA FROM THE AGRISAR CAMPAIGN

Wouter Dorigo [(1)], Heike Gerighausen [(2)]

[(1)]Institute of Photogrammetry and Remote Sensing (I.P.F.)
Vienna University of Technology (TU Wien)
Gusshausstrasse 27-29, 1040 Vienna, Austria
Email: wd@ipf.tuwien.ac.at

[(2)]German Remote Sensing Data Center
German Aerospace Center
Kalkhorstweg 53, 17235 Neustrelitz, Germany
Email: heike.gerighausen@dlr.de

ABSTRACT

This paper presents the results of automated extraction of crop characteristics from hyperspectral earth observation data. The data was acquired with an airborne AHS imaging spectrometer in the framework of the joint European AgriSAR 2006 campaign. The AgriSAR campaign was directed by the ESA and took place at the DEMMIN test site in northeast Germany, an agricultural area dominated by large monocultures. An important objective of this campaign was to establish to what degree novel radar and optical technologies are able to provide accurate agro-meteorological parameters for precision farming purposes.

Parameter retrieval in this study was performed with the CRASh approach, a software module based on the inversion of radiative transfer models. CRASh was developed at DLR as part of an automated operative processing chain for future hyperspectral missions. Validation of the model inversion results was performed with field measurements of leaf area index and leaf chlorophyll content which were carried out for winter wheat, winter barley, winter rape, maize, and sugar beet at two time steps during the 2006 growing season. Although spatial patterns of the model results generally coincide with the trends observed in the field, absolute accuracy of the fully automatically extracted variables appeared insufficient for precision agriculture purposes. The unsatisfying results are ascribed to a combination of causes, including angular anisotropy across the swath-width of the flight lines, the configuration of the applied bands, and the large number of model inversion solutions inherent to an automated environment in which little additional information on the observed canopy is present. Employing the airborne version of CRASh and incorporating a priori information on land cover and variable distributions is expected to drastically increase the retrieval performance.

KEYWORDS: hyperspectral, AHS, imaging spectroscopy, radiative transfer model inversion, CRASh, PROSPECT, SAILh, LAI, chlorophyll, winter wheat, winter barley, winter rape, maize, sugar beet

INTRODUCTION

The next generation of ESA Earth Observation satellites includes a series of ‘Sentinel Missions’ to be developed and operated within the framework of GMES (Global Monitoring for Environment and Security). These will include SAR and optical satellites with new imaging configurations and spectral bands, and much improved capabilities for frequent repeat coverage. The AgriSAR campaign was set up to collect in-situ, airborne SAR and optical measurements as well as satellite data in support of key issues relating primarily to the definition of Sentinel-1 but also Sentinel-2. The data base established in the course of AgriSAR will serve as an important basis in support of geophysical algorithm development, calibration and validation activities, and the simulation of future spaceborne earth observation missions. The increasing demand for value added products in the frame of GMES requires the development of automated procedures being integrated in automated processing chains to deliver data on the run.

The study presented in this paper makes use of the CRASh approach, a software module developed at DLR as part of an automated operative processing chain for future hyperspectral missions [1, 2]. CRASh relies on the inversion of radiative transfer models (RTMs). Compared to (semi-)empirical regression models based on vegetation indices, physically based RTMs have the advantage that they can be adapted to the prevailing observation geometry (view/sun constellation) and site specific characteristics such as local background reflectance, atmospheric conditions, crop type, and phenology. Moreover, RTMs offer the potential of exploiting the full information content contained in the

hyperspectral data. Nevertheless, due to strong correlation between many of the bands, even for such data the actual information dimensionality mostly lags far behind the number of bands offered by the earth observation system and, since a large range of canopy properties is responsible for similar variations in the spectral signature, the inverse problem usually has multiple solutions. This problem, which is common to RTM inversion in general, is often reduced by incorporating a priori information on canopy characteristics. As such, CRASh would gain most valuable results in a precision farming environment where well established data on the considered crops are available. However, in an operational processing chain such a priori information is usually absent and the solution has to come "all out of the data". To overcome the lack of a priori information in an automated environment, CRASh embodies several new techniques to address the information content contained within the hyperspectral data and to regularize multiple solutions.

In previous studies, CRASh has been tested for various types of imaging spectrometers, including the airborne HyMap sensor and the mutli-angular CHRIS/Proba sensor, and provided encouraging results for temperate grasslands and cotton fields in Uzbekistan [1, 2]. Goal of this paper is to test the performance of the automated CRASh mode for various common cash crops, including winter wheat, winter barley, winter rape, maize and sugar beet. For this purpose the approach will be employed to data collected with the Airborne Hyperspectral Scanner (AHS) in the framework of the AgriSAR 2006 campaign.

STUDY SITE AND DATA

Study Area

The AgriSAR campaign was carried out from April to July 2006 at the DEMMIN long-term test site (UL 54°2'54''N, 12°52'18''E; LR 53°45'40''N, 13°27'50''E), an intensively used agricultural area situated in the centre of Mecklenburg-Western Pomerania in Northeast Germany. The study presented in this paper concentrates on the Görmin farm, located in the north-eastern part of DEMMIN and covering about 2200 ha of cropland (Fig.1). The average field size in this area is very large with up to 180 ha per field. Main crops grown are winter wheat, winter barley, winter rape, maize and sugar beet. The topography of the area is very flat with only minor variations. Soil conditions are dominated by loamy to strong loamy sands.

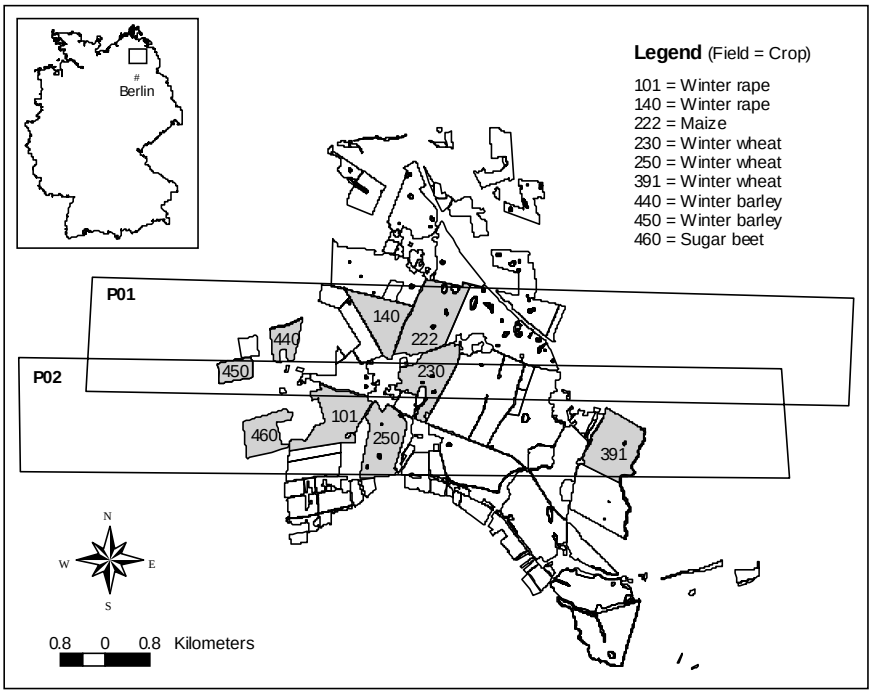

Fig.1. Overview of test site and the fields of the Görmin farm covered by AHS flightlines P01 and P02. Ground data applied on CRASh model approach was sampled on the fields coloured in grey.

AHS Data acquisition

Hyperspectral imagery was collected with the airborne AHS spectrometer on June 6 (12:57 (P02), 13:06 (P01) UTC) and July 4 2006 (8:58 (P02), 9:07 (P01) UTC) operated by the Instituto Nacional de Técnica Aerospacial, Spain (INTA). Due to the east-west flight direction, the relative azimuth between observation and sun position ranged between 45-51° (129-135°) in backward (forward) scattering direction (Tab.1). The spectrometer with a FOV of 90° was operated at a flight altitude of 991 m, resulting in a spatial resolution of 2.5 m at nadir. AHS covers 20 spectral channels in the VNIR and 43 in the SWIR.

The images were atmospherically corrected at INTAs by means of the ATCOR4 model [3]. Geometric correction was performed with PARGE [4]. For further analysis, all data sets were re-sampled to 6m resolution using nearest neighbour interpolation. Due to the low signal-to-noise ratio of several wavebands, particular in the SWIR, a spectral subset of 23 channels was selected (i.e., 455, 482, 510, 540, 569, 598, 627, 657, 686, 714, 743, 772, 801, 830, 860, 889, 917, 946, 976, 1003, 1553, 2033, 2046 nm).

Tab.1. Acquisition geometry for selected AHS imagery of AgriSAR 2006

	06.06.06		04.07.06	
	P01	P02	P01	P02
Solar zenith	39°	38°	39°	40°
Solar azimuth	228°	225°	131°	229°
True heading	270°	090°	090°	270°
Relative azimuth	48/132°	45/135°	51/129°	49/131°

Field and Lab Measurements

The canopy parameters that were sampled in the field during the AgriSAR campaign and applied in this study comprised leaf area index (LAI) and leaf chlorophyll a+b (Cab) content. Field measurements of these variables were collected on a weekly basis and during two intensive campaigns in June and July. The weekly measurements were undertaken by teams of the German Aerospace Centre-German Remote Sensing Data Centre (DLR-DFD) in cooperation with the Centre for Agricultural Landscape Research in Münchberg (ZALF) and the University of Kiel (CAU), while the intensive campaigns were performed by research groups of the Institute of intelligent systems for automation (ISSIA-CNR), University of Napoli (UNINA), University of Munich (LMU) and University of Valencia. During the weekly campaigns, LAI and chlorophyll samples were collected at 27 and 15 sampling units, in June and July respectively. These units were situated between farmers driving lanes and covered an area of approximately 9×9 m^2 around a marked GPS point. During the intensive campaigns in June and July, LAI and leaf chlorophyll were collected at respectively 12 and 208 additional sampling units where the size of sampling units were defined by each group separately.

Tab.2. Overview of variables, number of elementary sampling units (ESU), and sampling methods for each ground team at different dates of image data acquisition.

Team	LAI			Chlorophyll		
	# ESU		Sampling details	# ESU		Sampling details
	June	July		June	July	
DLR-DFD/ ZALF	15	15	Licor LAI2000; 2 meas. per SU	15	15	30 meas. per SU
CAU	12	12	Licor LAI2000; 2 meas. per SU	-	-	-
UNINA	-	14	Licor LAI2000; 24 meas.per SU	-	-	-
ISSIA	-	172	Decagon LP-80 AccuPAR; transects	-	-	-
LMU	6	11	4 meas. er SU	-	-	-
UV	-	-	Licor LAI2000; 24 meas. per SU	6	11	50 meas. per SU

Tab.3. Descriptive statistics of ground data used for model validation, separated according to crop type.

	June					**July**				
	Barley	Wheat	Rape	Maize	Sugar beet	Barley	Wheat	Rape	Maize	Sugar beet
Cab (µg/cm²)										
Min	35.50	36.60	36.25	13.66	26.80	-	39.90	26.46	26.40	32.90
Max.	46.04	40.89	37.45	23.19	31.95	-	45.70	28.43	39.20	44.50
Mean	42.50	38.21	36.71	18.01	29.30	-	43.25	27.32	34.48	39.03
St.dev.	4.83	1.64	0.65	4.82	2.12	-	2.99	1.01	4.44	3.79
LAI										
Min	4.07	3.84	4.32	-	-	3.03	2.37	3.09	0.92	0.10

Max.	5.89	5.80	5.75	-	-	4.36	8.22	3.85	2.28	4.24
Mean	5.02	4.54	5.01	-	-	3.40	4.53	3.40	1.69	1.65
St.dev.	0.63	0.54	0.65			0.49	1.42	0.28	0.33	0.57

LAI was sampled in a non-destructive way using the LICOR LAI-2000 and the Decagon's LP-80 AccuPAR instruments. Leaf chlorophyll content was measured in digital count units using the SPAD-502 DL (Minolta). For each sampling unit 30-50 measurements were acquired. Digital units were converted into chlorophyll concentrations (µg/cm²) via calibration functions from posterior instrumentation calibration. This was done by the University of Valencia who extracted chlorophyll samples during AgriSAR for determination in the lab using isocratic HPLC method based on [5]. Details on sampling methods for all teams and field data sets are summarized in Tab. 2, whereas summary statistics of the ground measurements are given in Tab.3.

RADIATIVE TRANSFER MODEL INVERSION BY CRASH

The CRASh approach

LAI and chlorophyll content were estimated from the geocoded and atmospherically corrected AHS data by employing the CRASh package [1, 2] . CRASh constitutes a modular approach for the inversion of radiative transfer models (RTM) and was particularly designed to operate within a (semi-)automated processing environment for imaging spectrometer data. The current version is based on the leaf- and canopy radiative transfer models PROSPECT [6, 7] and SAILh [8, 9]. Output of the CRASh inversion are the input vegetation variables used by PROSPECT and SAIlh for characterizing canopy reflectance in the forward mode, i.e. chlorophyll content (Cab), leaf water content (Cw), leaf dry matter content (Cdm), leaf brown pigment content (Cdm), leaf mesophyll structure index (N), leaf area index (LAI), average leaf angle (ALA), the hot spot parameter (HS), and soil brightness (BS). CRASh can operate in a completely automated mode or in a mode in which the user controls one or more inputs (e.g. land cover classification, prior knowledge on canopy characteristics, soil reflectance). This paper discusses the results that were obtained by the fully automated run of the model, so for the hypothetical situation that no a priori information on land cover or phenology is available.

Model inversion

In the automated mode, RTM inversion is accomplished on a per land cover basis, which means that both spectral characterization and model inversion itself are performed for each land cover class separately. The land cover classes are specified according to the rules proposed by SPECL [2, 10] and distinguish vegetation patches by vigorousness and development stage rather than by species. For each land cover class, non-systematic spectral uncertainty is calculated from the ensemble of pixels contained in the respective class and is for each waveband given by the standard deviation (σ). The inversion algorithm itself utilizes a minimization function based on lookup tables (LUTs). For each land cover class a separate LUT is generated according the expected variable ranges in the respective class. The reader is referred to [2] for an exhaustive overview of the applied variable distributions. The minimization algorithm searches for the closest spectral similarity between measured AHS reflectance (R_{meas}) and the reflectance in the class-specific LUT (R_{LUT}) using the cost function χ^2:

$$\chi^2 = \sum_{i=1}^{n_\lambda} \frac{(R^i_{meas} - R^i_{LUT})^2}{\sigma_i^2}$$

where n_λ is the number of wavebands. From the LUT, the 20% of spectra with the smallest χ^2 is selected. Based on this subset, the final solution is represented by the weighted average (see [1, 2] for further details).

RESULTS AND DISCUSSION

The validation of the CRASh approach concentrated on 9 fields grown with winter barley, winter wheat, winter rape, sugar beet, and maize where ground data had been sampled during or close to the time of airborne image data acquisition (see Fig.1). Model validation was performed by extracting average LAI and chlorophyll estimates from window of 3×3 pixels centred around the geographic position of the field sampling units.

Leaf Area Index

Fig. 2 shows estimated versus measured LAI for both acquisition days and flight lines. Results indicate a good model performance for the June data, with an RMSE less than 1 for flightline P01. At that date, the validated crops confined to winter barley, winter wheat and winter rape. The situation in July is somewhat different. LAI estimates correspond well with measured LAI values for maize and sugar beet but for all winter crops model estimates perform rather poor. A similar situation is apparent in Fig. 3 for field measurements collected during the intensive campaign by the various international partners. LAI values for maize and sugar beet are concentrated around the 1:1 line whereas for winter wheat LAI is conspicuously underestimated. Measurement errors for LAI are 11 % on average and as such can not justify the discrepancy with the estimated values.

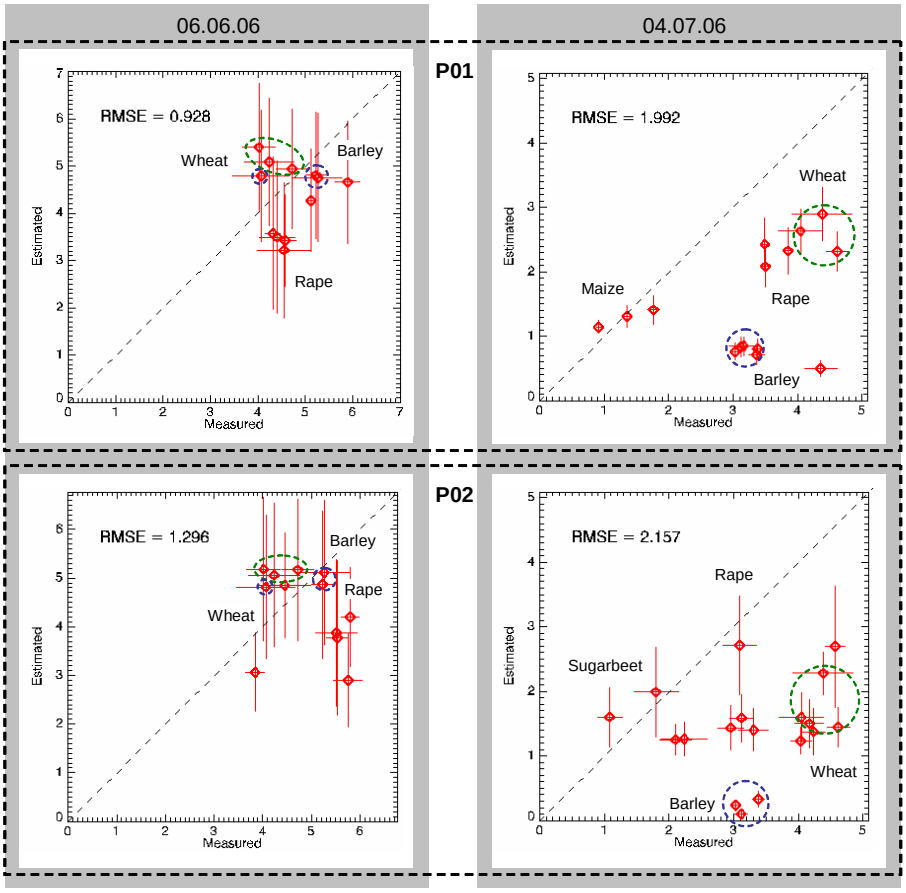

Fig.2. Estimated versus measured LAI values for ground truth during weekly measurements of DLR-DFD/ZALF and University of Kiel. Error bars indicate uncertainties of measured and estimated values.

Part of the bias between measured and estimated values can be explained by the non-destructive way of measuring LAI, as the employed instruments measure overall crop area index, including stems, ears, and senescent plant material, rather than merely the projected surface of green leaves. This may account to a significant overestimation of LAI, especially in the case of maturing fruits such as represented by winter wheat and barley in the July campaign. A second explanation has to be sought in the nature of canopy reflectance, since LAI and chlorophyll have a very similar effect on the spectrum in the visible wavelengths. In the absence of additional information, it remains unclear whether an increase (decrease) of radiation absorption is induced by increased (decreased) chlorophyll concentrations or by a denser (less dense) canopy, both leading to a very similar spectral shape. Thus, using the automated RTM inversion which in this case is principally based on VIS wavebands, low LAI estimates should be compensated by high chlorophyll concentrations and vice versa. This trend is confirmed by the results obtained for chlorophyll presented in the next paragraph.

Due to an overlap between the two flight lines of about 800 m in width, a doubled set of model estimates were available for field 230 (winter wheat) and 450 (winter barley). According data points are encircled in Fig.2. Whereas results coincide very well for June, LAI values estimated from the July data set differ about a factor 1.5 for the consecutive flightlines. Ground measurements generally agree better with model estimates for flightline 1 which is confirmed by the RMSE value. A plausible explanation for the deviations observed for the July data set is the strong spectral anisotropy caused by the changing observation angle. The flight lines had not been corrected for such anomalies neither had CRASh been adapted to account for different observation angles within a single scan line.

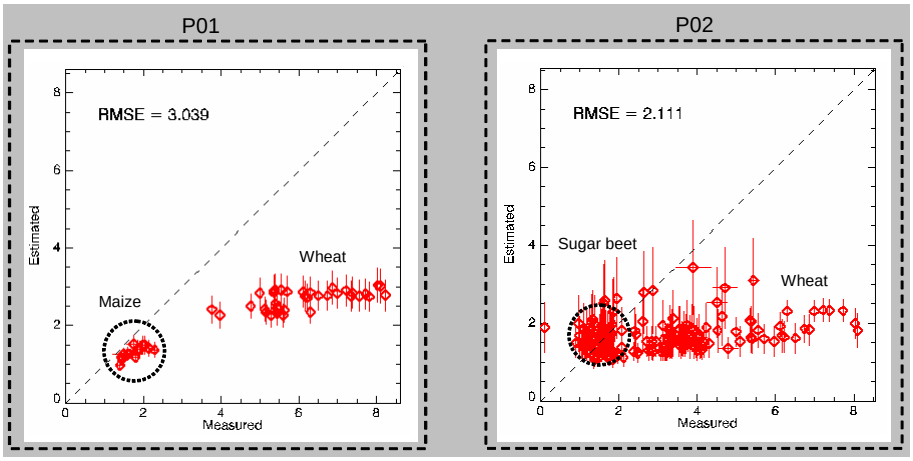

Fig.3. Estimated versus measured LAI values for ground truth during 3rd intensive campaign in July by various international partners. Left: flighline P01, right: P02

To assess model results with respect to canopy development over time, a comparison of LAI values from June to July has been plotted in Fig.4. Positive differences indicate an increase from June to July, negative values point out a decrease. The four black bars show the differences of estimated LAI values based on flightline 2. Analogous to the results presented in Fig.2, there is little agreement for absolute values, but the plot confirms the same general tendency for model results and ground measurements, with three sample units of wheat and rape being the only exception. Because crops were not yet growing in June, no comparison could be drawn for maize and sugar beet.

Leaf chlorophyll a+b

Calibration functions for SPAD-502 were supplied by the University of Valencia as a general function for both instruments used, SPAD A and B. In addition, crop-specific calibration functions were supplied for SPAD B instrument (Tab.4). These different functions were applied to SPAD digital counts (DC) to constitute the chlorophyll concentrations in µg/cm² (Cab) used for model validation. When applying general or crop-specific functions (Tab.5), in terms of RMSE, the calibrated SPAD values neither lead to a significant improvement nor to a major degradation of the model validation results. Estimated and measured values partially differ about a factor 2, a deviation that can neither be explained by crop-specific or instrument specific calibration functions nor by the measurement errors inherent to the field data which is on average 10% for chlorophyll measurements. In fact, estimated Cab agrees better with measured SPAD DC than with calibrated chlorophyll concentrations (Tab.5). A similar phenomenon has been observed by [1] for chlorophyll estimates of cotton leaves. Comparing chlorophyll concentrations from the AgriSAR-campaign with chlorophyll concentrations measured during other campaigns, it becomes evident that data variability is rather low in the AgriSAR data set [11], which hampers distinguishing trends and establishing regressions between estimated and measured values.

Tab.4. SPAD-502 instrument calibration functions for determination of chlorophyll concentrations supplied by University of Valencia. DC = SPAD digital count.

Specification	Calibration functions	R^2
Universal-B (SPAD B)	0.722 x DC	0.76
Universal-A (SPAD A)	0.859 x DC	0.69
Maize (SPAD B)	0.703 x DC	0.81
Barley (SPAD B)	0.730 x DC	0.67

Wheat (SPAD B)	0.769 x DC	0.88
S.-Beet (SPAD B)	0.695 x DC	0.43

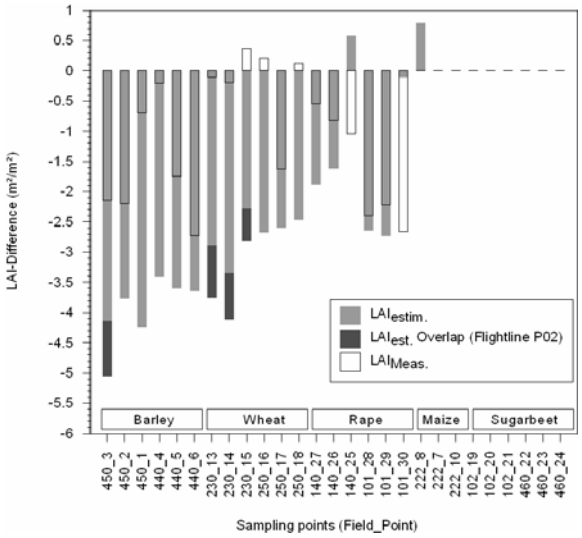

Fig.4. Temporal evolution of estimated and measured LAI-values displayed as the difference between data acquisition in June and July. Positive values indicate increasing LAI values from June to July. Negative values show a decrease of LAI from June to July.

Tab.5. RMSE of estimated vs. measured values for chlorophyll concentrations based on general and crop-specific calibration functions and on raw SPAD digital counts.

RMSE		**06.06.06**			**04.07.06**		
		General	Crop-specific	SPAD DC	General	Crop-specific	SPAD DC
P01	Weekly	35.1	-	30.2	36.3	-	30.3
	Intensive	47.6	45.6	33.4	45.3	45.1	31.8
P02	Weekly	42.2	-	35.3	29.3	-	22.0
	Intensive	n.d.	n.d.	n.d.	39.8	41.2	25.5

Analysing spatial patterns

To exemplarily illustrate the spatial distribution of LAI and Cab as estimated by CRASh, the results for fields 140, 222, and 230 in July have been plotted in Figs. 5 and 6. Natural distinctions between the different field crops winter rape, maize, and winter wheat are clearly recognizable. LAI for maize is lowest owing to its early growth stage and plant structure. In contrast, plant growth of winter crops is almost completed at the beginning of July when spikes start to develop, which is expressed by LAI values. Similarly, crop specific differences in chlorophyll concentrations become apparent. Despite low LAI, chlorophyll concentrations are high for maize because of green fresh plant material which is confirmed by the ground measurements. Inside the fields considerable variations of parameters can be observed. On the one hand, this is accounted for by the farmers driving lanes. They draw distinctive directional structures either running east-west or northeast-southwest in all plots. Other non-directional variations are attributed to natural inhomogeneities resulting from the local water and nutrient availability due to relief and soil conditions.

As described before, a small amount of a priori information on canopy parameters is retrieved from the embedded automatic land cover classification with SPECL. Four land cover classes were identified for the example displayed in Fig.5. Although no general dependency between the SPECL classification and canopy estimates was observed for the validation with field measurements, the spatial distributions do reveal a slight interdependency of LAI and Cab estimates and the respective land cover classes.

The model inversion applied in this study did not account for angular spectral anisotropy across the FOV. The influence of spectral anisotropy on model inversion is twofold: on one hand it influences land cover classification of SPECL which is based on nadir reflectance template spectra. This effect can be well studied in the upper left part of field 140 in Fig.5. On the other hand, typical smooth transitions, i.e. a steady increase or decrease in LAI or Cab occur on some fields in the swath direction of the sensor. An improvement is expected by using the airborne version of CRASh which includes both nadir normalization of the reflectance data prior to land cover classification and RTM

inversion being performed separately for different view angle intervals (see [1, 2] for further details). As can be seen in Fig.6, the influence of spectral anisotropy on model results is highest on the outer margins of two overlapping flight lines where largest discrepancy between view directions exists.

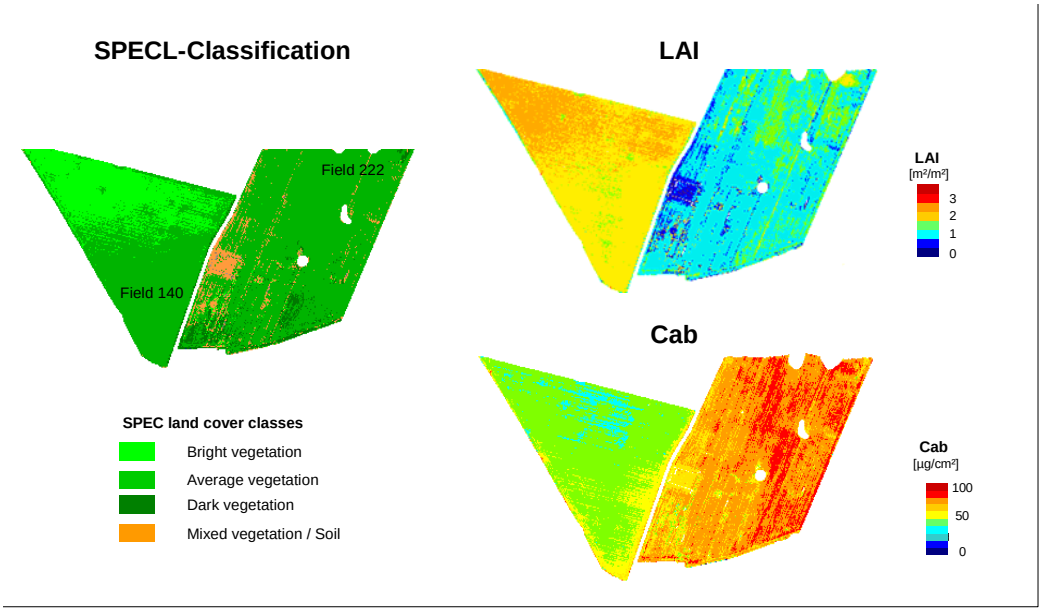

Fig.5. SPECL land cover classification results and estimated LAI and Cab for fields 140 (winter rape) and 222 (maize) based on AHS image data from 04.07.2006 for flightline P01.

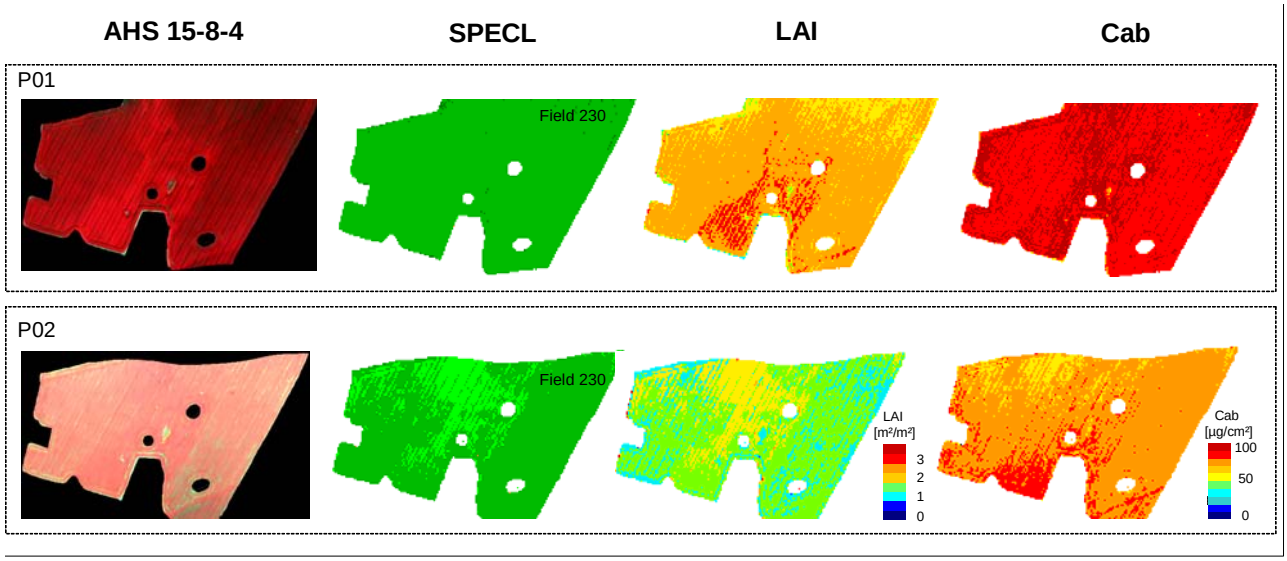

Fig.6. Results of CRASh approach for field 230 (winter wheat) based on flightline P01 and P02 in July. Differences are supposed to result from spectral angle effects. For the legend of the SPECL classification see Fig.5.

CONCLUSIONS AND OUTLOOK

This paper presented the results of automated LAI and leaf chlorophyll retrieval from hyperspectral AHS data using the CRASh approach. The results were validated with field data that were collected in the framework of the AgriSAR 2006 campaign for winter wheat, winter barley, winter rape, maize, and sugar beet. Although the results well mimicked the spatial and temporal variations between the different crops, absolute accuracy was too low to allow for consistent incorporation of the results in spatially distributed crop growth models used in the context of precision agriculture. The origin of the reported inconsistencies resides both in the prepocessing of the data (calibration, atmospheric correction,

BRDF correction), as well as in the parameterization of the RTM inversion (e.g., band selection, accounting for spectral anisotropy across swath-width of sensor, definition of LUTs). Regarding the latter, it is expected that significant additional improvement can be obtained by employing a detailed crop map and incorporating a priori information on the crop canopy variables available through field measurements. This will allow optimizing model inversion for the considered crop types and phenology and confine the range of possible solutions. After all, this is a realistic scenario in the context of precision agriculture applications where crop type and growth stadium are very well known in advance and the farmer's primary interest is to distinguish intrafield variations in crop development.

ACKNOWLEDGEMENTS

All model results presented in this publication base on airborne image data and on field data acquired during the AgriSAR 2006 campaign, funded by the European Space Agency (ESA).
The authors are grateful to the team from ZALF for their close cooperation with the DLR-DFD during weekly measurements, including the support of measuring devices and lab facilities. We would like to thank all members of the ground teams from ZALF, CAU, LMU, UNINA, University of Valencia, and ISSIA for their painstaking work in the field and subsequent provision of their field data for analysis. INTAS is greatly thanked for the provision of AHS image data. Thanks are addressed in particular to Eduardo de Miguel and Jose Antonio Gomez for image processing. Mrs. Soledad Gandia from University of Valencia is thanked for placing at disposal SPAD chlorophyll calibration functions.

REFERENCES

[1] W.A. Dorigo, F. Baret, R. Richter, G. Ruecker, M. Schaepman, and A. Mueller, "Retrieving canopy variables by radiative transfer model inversion - an automated regional approach for imaging spectrometer data," in: I. Reusen and J. Cools (Editors), 5th EARSeL SIG IS Workshop on Imaging Spectroscopy, Brughes, Belgium, April 2007.
[2] W.A. Dorigo. Retrieving canopy variables by radiative transfer model inversion - a regional approach for imaging spectrometer data, PhD Thesis, Technical University of Munich, pp. 258, 2007.
[3] R. Richter and D. Schlaepfer, "Geo-atmospheric processing of airborne imaging spectrometry data. Part 2: atmospheric/topographic correction," International Journal of Remote Sensing, 23(13): pp. 2631-2649, 2002.
[4] D. Schlaepfer and R. Richter, "Geo-atmospheric processing of airborne imaging spectrometry data. Part 1: parametric orthorectification," International Journal of Remote Sensing, 23(13): pp. 2609-2630, 2002.
[5] J. de las Rivas, A. Abadía and J. Abadía, "A new reversed phase HPLC method resolving all major higher plant photosynthetic pigments," Plant Physiology, 91, pp. 190-192, 1989.
[6] T. Fourty, F. Baret, S. Jacquemoud, G. Schmuck, and J. Verdebout, "Leaf optical properties with explicit description of its biochemical composition: Direct and inverse problems," Remote Sensing of Environment, 56(2): pp. 104-117, 1996.
[7] S. Jacquemoud and F. Baret, "PROSPECT: A model of leaf optical properties spectra," Remote Sensing of Environment, 34(2): pp. 75-91, 1990.
[8] W. Verhoef, "Light scattering by leaf layers with application to canopy reflectance modeling: The SAIL model," Remote Sensing of Environment, 16(2): pp. 125-141, 1984.
[9] W. Verhoef, "Earth observation modeling based on layer scattering matrices," Remote Sensing of Environment, 17(2): pp. 165-178, 1985.
[10] R. Richter, "Atmospheric / Topographic Correction for Airborne Imagery, ATCOR-4 User Guide, Version 4.2," DLR - German Aerospace Center, Remote Sensing Data Center, 2007.
[11] S. Gandia, pers. comm. (see also this issue), 2007.